Limnol. Oceanogr., 53(4), 2008, 1548–1561

Heat budget and thermal microenvironment of shallow-water corals: Do massive corals get warmer than branching corals?

Isabel M. Jimenez
Institute for Water & Environmental Resource Management, Department of Environmental Science, University of Technology, Sydney, Broadway, New South Wales 2007, Australia

Michael Kühl
Marine Biological Laboratory, Department of Biology, University of Copenhagen, Strandpromenaden 5, DK-3000 Helsingør, Denmark

A. W. D. Larkum
School of Biological Sciences, Heydon-Laurence Building A08, University of Sydney, New South Wales 2006, Australia

P. J. Ralph[1]
Institute for Water & Environmental Resource Management, Department of Environmental Science, University of Technology, Sydney, Broadway, New South Wales 2007, Australia

Abstract

Coral surface temperature was investigated with multiple temperature sensors mounted on hemispherical and branching corals under (a) artificial lighting and controlled flow; (b) natural sunlight and controlled flow; and (c) in situ conditions in a shallow lagoon, under naturally fluctuating irradiance, water flow, and temperature. Under high irradiance and low flow conditions, hemispherical corals were 0.6°C warmer than the surrounding water. Hemispherical corals reached higher temperatures than branching corals, by a measure of 0.2°C to 0.4°C. Microsensor temperature measurements showed the presence of a thermal boundary layer (TBL). The TBL thickness was flow dependent, and under low flow conditions, a TBL up to 3 mm thick limited heat transfer to the ambient water. Combined microsensor measurements of temperature and oxygen showed that the TBL was approximately four times thicker than the diffusive boundary layer, as predicted from heat and mass transfer theory. A simple conceptual model describes coral surface temperature as a function of heat fluxes between coral tissue, skeleton, and surroundings. The slope of the predicted linear relationship between coral temperature and solar irradiance is fixed by the efficiencies of light absorption and the heat losses to the skeleton and the water. Although spectral absorptivity may play a significant role in coral warming, shape-related differences in thermal properties can cause hemispherical corals to reach higher temperatures than branching corals. Shape-related differences in thermal histories may thus help explain differences in susceptibility to coral bleaching between branching and hemispherical coral species.

[1] Corresponding author (Peter.Ralph@uts.edu.au).

Acknowledgments

We thank N. Ralph for constructing the flow-through chamber and R. Bilger and J. Kent for valuable discussion of heat transfer theory. We thank M. Ball for discussions of heat transfer in corals at an early stage of this investigation and two anonymous reviewers for their valuable comments. We acknowledge the Department of Environmental Sciences, University of Technology, Sydney, and all staff at Heron Island Research Station for support.

This research was funded by a University of Technology, Sydney, institutional grant to P.J.R.; by the Australian Research Council (P.J.R. and M.K.); and by a grant from the Danish Natural Science Research Council (to M.K.). The research was conducted under Great Barrier Reef Marine Park Authority permits G05/16166.1, G03/12019.1, and G06/178151.

This is contribution 219 from the Institute of Water and Environmental Resource Management and contribution 0007 from the Sydney Institute of Marine Science.

The increasing occurrence of coral bleaching over the last two decades has focused attention on temperature fluctuations on corals reefs (Brown 1997; Berkelmans and Willis 1999; Hoegh-Guldberg 1999). Under mass coral bleaching conditions, small excursions in the ambient water temperature on a coral reef (of just a few degrees Celsius above the normal average temperature maximum) induce the expulsion of the endosymbiotic dinoflagellates (zooxanthellae) and/or the loss of pigments from a wide variety of corals (Glynn 1996; Hoegh-Guldberg 1999). If such high temperature anomalies last for a week or more mass mortality of corals can occur (Glynn 1996; Hoegh-Guldberg 1999; Coles and Brown 2003).

In most of the literature on coral bleaching, temperature of the ambient water is always assumed to be the same as the coral temperature. However, as a result of the shallow nature of many coral reef lagoons, radiant energy reaching the coral surface can increase its temperature relative to the surrounding water. Few studies have considered the

temperature of corals and the heat fluxes at their surface. Brown et al. (2002) investigated the temperature of different surfaces of air-exposed corals but found no differences. Fabricius (2006) measured the surface temperature of a number of shallow-water corals and showed that more densely pigmented corals heated up more than did less densely pigmented corals, an effect that was enhanced under low water flow. The latter study provides qualitative evidence that heat fluxes at the surface of corals can play an important role in the microscale physical processes involved in coral bleaching. However, the study provides no quantitative data on which a model of heat fluxes could be established, and, in particular, it does not differentiate between large massive corals (that are roughly hemispherical in shape) and thin, branching corals.

The aims of this study were to better understand heat fluxes and microscale temperature dynamics in corals and to investigate differences in thermal characteristics between branching and hemispherical corals. We use a heat budget model of a coral to describe surface warming in both steady state and transient state, in terms of the relevant heat fluxes (radiation, convection, and conduction) as well as the coral's geometrical parameters (surface area to volume ratio). Our simple mathematical model is supported by experimental data, including the first detailed measurements of the thermal microenvironment of corals. The thermal boundary layers of corals were investigated and compared to the analogous and better-documented diffusive boundary layer for oxygen (Shashar et al. 1993; Kühl et al. 1995). The temperature dynamics of branching and hemispherical corals were explored both in controlled laboratory experiments and on the reef flat under naturally fluctuating conditions of flow and irradiance.

Theoretical considerations

In view of recent evidence that the surface temperature of a coral is not always equal to that of the surrounding water (Fabricius 2006), it becomes imperative to distinguish between the temperature of (1) the thin layer of living tissue embedded in the surface of a coral that is exposed to direct solar radiation, (2) the ambient water, and (3) the coral skeleton. In order to predict the extent of coral warming and to understand the role of environmental fluctuations in irradiance, water flow, and temperature, we first describe a theoretical heat budget of a coral.

Heat budget of a coral exposed to solar radiation and water flow

Coral tissue is a continuous pigmented layer on the outer surface of a calcareous skeleton and is exposed to direct solar radiation. We therefore divide the coral into two distinct thermal regions (*see* Fig. 1a): A portion of coral tissue that intercepts the direct solar beam (at temperature T_{tissue}) and the remaining coral, which includes the underlying skeleton and the shaded tissue (at temperature T_{skel}). We describe a heat budget for both thermal regions and derive expressions for T_{tissue} and T_{skel}. The relevant energy fluxes are the absorption of

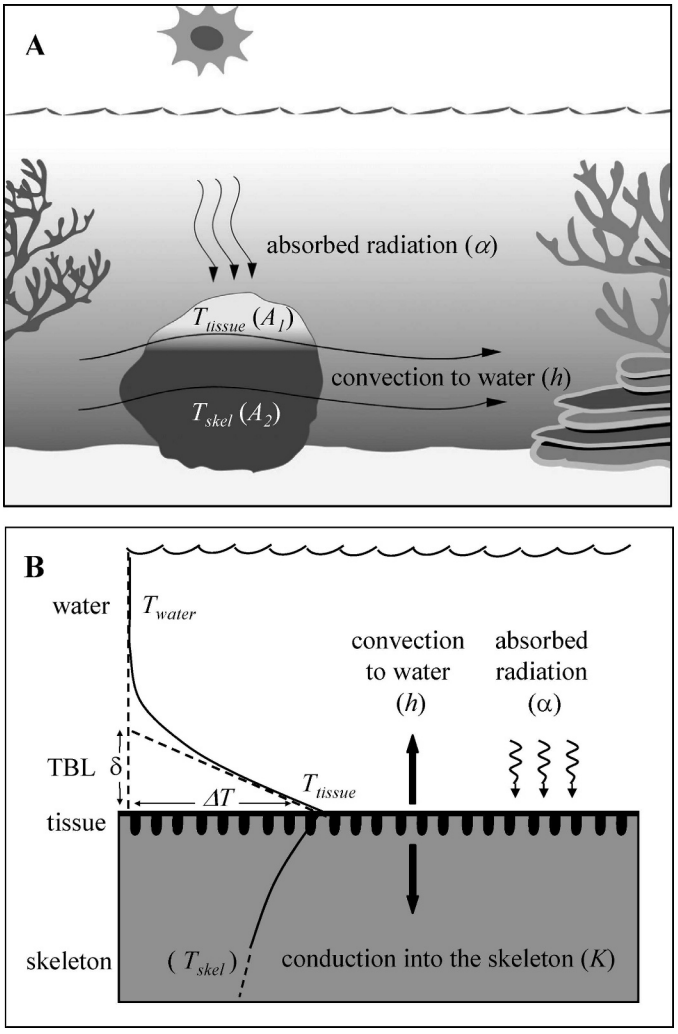

Fig. 1. Conceptual diagrams of the relevant heat fluxes (and associated parameters) in (a) a whole coral divided into sun-exposed and shaded regions (of surface areas A_1 and A_2, respectively) and (b) in a small portion of surface tissue: radiation absorption (absorptivity, α); heat loss to the skeleton by conduction (skeleton conductance, K); heat loss to the water column by convection (convection coefficient, h). Schematic temperature profile, where T_{tissue} is the coral tissue temperature, T_{water} is the water temperature away from the boundary layer, and T_{skel} is the skeleton core temperature. Definition of the effective thickness (δ) of the thermal boundary layer [TBL], where ΔT is the coral surface warming ($T - T_{water}$).

incident solar radiation by the exposed tissue (q_{rad}), the conduction of heat to the underlying skeleton (q_{cond}), and the convection heat loss to the water, from the heated tissue (q_{conv1}) and from the remaining coral (q_{conv2}), expressed in W m^{-2} (*see* Fig. 1a,b). The heat budget (e.g., Incropera and DeWitt 1996) for each region is (assuming an infinitely thin layer of tissue, thus, with zero heat capacity)

Tissue heat budget :

$$0 = A_1 q_{rad} - A_1 q_{conv1} - A_1 q_{cond} \qquad (1)$$

Table 1. List of terms.

α	Tissue absorptivity	m	Scaling exponent
δ	Boundary layer thickness	Nu	Nusselt number
ε	Surface emissivity	PAR	Photosynthetically active radiation
ρ	Skeleton density (kg m^{-3})	q_{rad}	Absorbed radiation flux (W m^{-2})
σ	Stefan–Boltzmann constant	q_{cond}	Conduction flux from the tissue to the skeleton (W m^{-2})
τ	Transient response time (s)	q_{conv1}	Convection flux from the sun-exposed tissue to the water (W m^{-2})
ΔT	Warming: $T - T_{water}$ (K or C)	q_{conv2}	Convection flux from the shaded tissue to the water (W m^{-2})
$\Delta T_{m\,tissue}$	Maximum surface warming (K or C)	Re	Reynolds number
$\Delta T_{m\,skel}$	Maximum skeleton warming (K or C)	TBL	Thermal boundary layer
A_1	Surface area of sun-exposed tissue (m^2)	T_{tissue}	Tissue temperature (K)
A_2	Surface area of shaded tissue (m^2)	T_{skel}	Skeleton temperature (K)
A	Total coral surface area (m^2)	T_{water}	Water temperature (K)
c	Skeleton specific heat capacity (J kg^{-1} K^{-1})	V	Coral volume (m^3)
DBL	Diffusive boundary layer		
E	Incident irradiance (W m^{-2})		
h	Convection coefficient (W m^{-2} K^{-1})	Model constants	
k	Conductivity (W m^{-2} K^{-1})	K_0	$1 + 1/(A_1/A_2 + h/K)$
K	Skeleton conductance (W m^{-2} K^{-1})	K_1	$(KA + hA_2)/KA_1$
Le	Lewis number	K_2	$K_0K/K_1(K + h)$
		K_3	$(K + hA_2/A)/(K + h)$

Skeleton heat budget :

$$\rho cV\, dT_{skel}/dt = A_1 q_{cond} - A_2 q_{conv2} \qquad (2)$$

where ρ, c, and V are the skeleton's density, specific heat capacity, and volume, respectively; dT_{skel}/dt is the variation in skeleton temperature ($\rho cV\, dT_{skel}/dt$ is the variation in heat stored within the coral skeleton); and A_1 and A_2 are the surface areas of exposed and shaded tissue, respectively (*see* Fig. 1a). Positive values of q_{conv1}, q_{conv2}, and q_{cond} indicate a convective heat flux toward the water and a conductive heat flux from the tissue to the skeleton, respectively. Expressions for each heat transfer term in Eqs. 1 and 2 are listed in Tables 1 and 2.

Absorbed radiative heat flux—The heat flux due to absorption of radiation, q_{rad}, is proportional to the incident solar irradiance (E), the surface area of exposed tissue (A_1), and the tissue absorptivity (α) (Table 2; Eq. 3). Defined as the fraction of incident radiation absorbed by the surface, α accounts for a range of factors affecting the amount of absorbed light, such as the optical properties of both the host tissue (host pigments, tissue thickness) and the zooxanthellae (symbiont density, photosynthetic pigments). For purposes of simplification, we treat the tissue layer as a homogeneous absorbing medium and neglect local heterogeneity that arises from the structural organization of host and symbiont cells and pigments, as well as the coral skeleton (Kühl et al. 1995; Enriquez et al. 2005).

Convective heat loss to the surrounding water—The convective heat transport, q_{conv1}, and q_{conv2} obey Newton's law of cooling (Incropera and DeWitt 1996) and are proportional to the difference in temperature between the water (T_{water}) and the coral (T_{tissue} and T_{skel}, respectively), the surface area of exchange (A_1 and A_2, respectively), and the convection coefficient h (W m^{-2} K^{-1}) (Table 2; Eqs. 4 and 6). h accounts for the effects of flow rate, flow type (laminar or turbulent), and effects of coral morphology on local shear stress (e.g., Gates 1980; Denny 1993).

Conduction of heat to the skeleton—The heat conduction, q_{cond}, is proportional to the temperature difference between the surface T_{tissue} and the skeleton T_{skel}, the surface area of exchange (A_1), and the conductance of the skeleton K (W m^{-2} K^{-1}) (Gates 1980) (Table 2; Eq. 5).

Thermal radiation—The net radiative heat flux from a surface at temperature T surrounded by a transparent medium at temperature T_1 is given by the Stefan–Boltzmann law: $q = \varepsilon\sigma(T^4 - T_1^4)$, where ε is the surface emissivity and σ is Stefan–Boltzmann's constant, (5.67×10^{-8} W m^{-2} K^{-4}). For corals submerged in water that heavily absorbs long-wavelength radiation and radiates

Table 2. Heat transfer terms used in the model (after Incropera and DeWitt 1996).

Thermal region	Definition	Equation	Eq.
Sun-exposed tissue (surface area A_1)	Absorbed radiation	$q_{rad} = \alpha E$	3
	Convection to water	$q_{conv1} = h(T_{tissue} - T_{water})$	4
	Conduction from the tissue to the skeleton	$q_{cond} = K(T_{tissue} - T_{skel})$	5
Skeleton (surface area A_2)	Conduction from the tissue to the skeleton	$q_{cond} = K(T_{tissue} - T_{skel})$	5
	Convection to water	$q_{conv2} = h(T_{skel} - T_{water})$	6

back to the coral, the exact calculation is more complex, but it will not exceed the value given by the Stefan–Boltzmann law (i.e., approximately 5 W m^{-2} for a coral at 28°C in water at 27°C, and assuming a large emissivity [ε = 0.9]). In comparison, the convective heat loss would be 300 W m^{-2} for the same temperature difference and assuming a convection coefficient (h) of approximately 300 W m^{-2} K^{-1} (a realistic value for a sphere or cylinder 50 mm in diameter, in a 1 cm s^{-1} flow; Incropera and DeWitt 1996). Thus, thermal radiation is less than 2% of convection heat loss and can be left out of our model, which greatly simplifies its mathematical formulation.

Solutions of the heat budget equations—Combining Eqs. 3 to 6 (Table 2) into the heat budgets (Eqs. 1 and 2) results in the following:

$$T_{tissue} - T_{water} = (T_{skel} - T_{water})K/(K + h) + E\alpha/(K + h) \quad (7)$$

$$\rho cV\, dT_{skel}/dt = -(T_{skel} - T_{water})(KA_1 + hA_2) + (T_{tissue} - T_{water})KA_1 \quad (8)$$

Inserting Eq. 7 into Eq. 8 and solving for T_{skel} results in

$$T_{skel} = T_{water} + \Delta T_{m\,skel}\left(1 - e^{-t/\tau}\right) \quad (9)$$

$$\Delta T_{m\,skel} = E\alpha/K_1 h \quad (10)$$

$$\tau = (\rho cV/AK_3 h) \quad (11)$$

where K_1 and K_3 are constants equal to $(KA + hA_2)/KA_1$ and $(K + h\ A_2/A)/(K + h)$, respectively (Table 1); $\Delta T_{m\,skel}$ is the maximum warming of the bulk skeleton (i.e., maximum difference between T_{skel} and T_{water}), and τ is a constant with the dimension of time.

Inserting Eq. 9 into Eq. 7 and simplifying the mathematical formulation provides the coral surface temperature, thus:

$$T_{tissue} = T_{water} + \Delta T_{m\,tissue}\left(1 - K_2 e^{-t/\tau}\right) \quad (12)$$

$$\Delta T_{m\,tissue} = E\alpha/K_0 h \quad (13)$$

where K_0 and K_2 are constants equal to $1 + 1/(A_1/A_2 + h/K)$ and $K_0K/(K_1(K + h))$, respectively (Table 1); and $\Delta T_{m\,tissue}$ is the maximum warming of the exposed tissue layer (i.e., maximum difference between T_{tissue} and T_{water}).

Equations 9 and 12 describe the thermal response of coral skeleton and surface, respectively, in a transient state (i.e., directly following a sudden change in environmental conditions, such as an increase in radiation). Equations 10 and 13 provide the steady-state difference in temperature between coral skeleton and water and between coral tissue and water, respectively (i.e., the temperature difference reached when environmental conditions are held constant for an extended period of time). The equations simply state that the absorption of radiative heat drives an increase in surface temperature, and this is counter-balanced by convection to the surrounding water and depends on the relative importance of convection and conduction (h/K, via K_0).

The solutions to our model for transient (Eqs. 9 and 12) and steady (Eqs. 10 and 13) states enable prediction of the coral temperature, given a prescribed set of environmental conditions (irradiance, E; water temperature, T_{water}; and flow, via convection, h) and a specific set of coral parameters: α, K, ρ, c, V, A_1, and A_2. In particular, the convection coefficient (h) reflects the complexity of convective heat transfer in that it is affected by the characteristics of the fluid flow (velocity, turbulent or laminar) and by the geometry of the coral (shape and size) (e.g., Patterson 1992; Incropera and DeWitt 1996). This complexity is due to thermal boundary layers that form at the surface of objects immersed in a moving fluid and that control heat fluxes between bodies and the surrounding medium (Gates 1980).

Diffusive and thermal boundary layers

The thermal boundary layer (TBL) at the surface of a submerged object is analogous to the diffusive boundary layer (DBL) in that they both emerge through the action of viscous forces in the fluid (Dade et al. 2001) and limit the exchange of heat and solutes (such as oxygen) between the surface and the free stream. Exchange of dissolved gases and nutrients between aquatic organisms and the surrounding water is especially important for metabolism, and, consequently, much attention has focused on the effect of flow on mass transfer across the DBL (Jørgensen 2001) for coastal sediments (Jørgensen and Revsbech 1985), microbial mats (Jørgensen and Des Marais 1990), seagrasses (Koch et al. 2006), and corals (Shashar et al. 1993; Lesser et al. 1994; Kühl et al. 1995). Small water velocities and accompanying large DBLs of corals limit photosynthesis and respiration rates (Dennison and Barnes 1988; Shick 1990; Finelli et al. 2006) and affect nutrient uptake (Atkinson and Bilger 1992) and prey capture (Patterson 1991). In contrast, the thermal boundary layers of corals have not been investigated. Fabricius (2006) showed that coral surface warming was reduced at high flow rates and suggested that water flow contributed to cooling corals by thinning the TBL. Here we use the theory of heat transfer and the analogy between TBL and DBL to describe a method for calculating the convection heat flux (q_{conv}) and the convection coefficient (h) from measured temperature profiles in the TBL. In light of the heat–mass transfer analogy we consider it useful to show the relative scale of TBL and oxygen DBL in corals.

Heat and oxygen flux across the thermal and diffusive boundary layers

Within the boundary layer, water flow is streamlined, with very little vertical mixing (Gates 1980); thus, diffusion rather than advection dominates the transport of heat and oxygen. Immediately next to the coral surface, the convective heat flux q_{conv} (q_{conv1} and q_{conv2}; Table 1) equals

a conductive heat flux in water (not to be confused with q_{cond} in the skeleton) and is described by Fourier's law of conduction (Gates 1980). Heat and mass transfer are analogous physical processes, and the flux of oxygen across the DBL is described by an identical mathematical formulation, Fick's first law of diffusion. Thus, the flux of heat, q_{conv}, and oxygen, J, to the water is proportional to the gradient of temperature, T, and oxygen concentration, C, at the surface, so that

$$\text{Surface heat flux: } q_{conv} = -k\frac{dT}{dz} \quad \text{at } z = 0 \quad (14)$$

$$\text{Surface oxygen flux: } J = -D\frac{dC}{dz} \quad \text{at } z = 0 \quad (15)$$

where z is the direction normal to the surface and oriented toward the water, k is the thermal conductivity of water (0.616 W m^{-1} K^{-1}; Denny 1993), and D is the diffusion coefficient of oxygen in water (1.98×10^{-9} m^2 s^{-1} for air-saturated seawater at 25°C; Larkum et al. 2003). The surface temperature gradient in Eq. 14 can, alternatively, be expressed in terms of the temperature difference ($T - T_{water}$) and the thickness of the effective TBL, δ (defined in Fig. 1b, in analogy with the definition of the thickness of the effective DBL by Jørgensen and Revsbech 1985). Equation 14 thus becomes

$$q_{conv} = k\frac{T - T_{water}}{\delta} \quad (16)$$

Substituting q_{conv}, k, and T with J, D, and C, respectively, provides the counterpart of Eq. 16 for mass transfer, which is commonly used for oxygen flux determination across the DBL of aquatic organisms (Jørgensen and Des Marais 1990; Larkum et al. 2003).

Combining Eq. 4 (Table 2) and Eq. 16 produces the convection coefficient (h) and shows the inverse relationship between the thickness of the thermal boundary layer (δ) and the efficiency of convective heat transfer, thus:

$$h = \frac{k}{\delta} \quad (17)$$

Materials and methods

Corals—Samples were collected in the Heron Island lagoon adjacent to Heron Island Research Station (151°55′E, 23°26′S) in January 2006 and were maintained in continuously flowing seawater (26°C—ambient lagoon temperature) overnight before commencement of the experiment. Seven individual corals were used to investigate the coral temperature microenvironment (individual hemispherical colonies: *Favia* sp. (~35 mm in diameter), *Cyphastrea serailia* (~50 mm), *Favia rotunda* (~90 mm), *Porites lobata* (~35 mm); individual branches: *Porites cylindrica* (~4 mm), *Stylophora pistillata* (~6 mm), *Seriatopora hystrix* (~3 mm). Four hemispherical colonies of *P. lobata* (30–40 mm in diameter) and four branching colonies of *S. pistillata* (branch thickness, 5–6 mm) were used for solar heating experiments. Four hemispherical colonies of *C. serailia* (~50 mm in diameter) and four branching colonies of *P. cylindrica* (branch thickness, ~10 mm) were used for in situ monitoring of coral temperature.

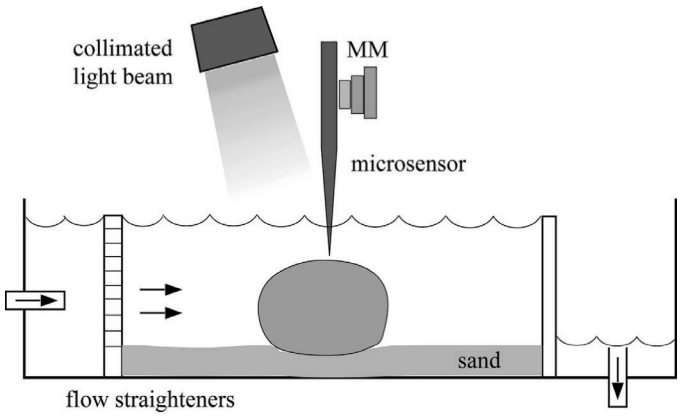

Fig. 2. Diagram of experimental setup used for measurements of temperature and oxygen microenvironment. The temperature microsensor was mounted on a motorized micromanipulator (MM) and connected to a thermocouple meter (*see* text). For the O_2 profiles, the temperature microsensor was replaced by an O_2 microelectrode connected to a picoamperemeter (*see* text).

Temperature microenvironment—Corals were placed in a flow chamber (Plexiglas, 10 × 5 × 25 cm), in which illumination was provided by a fiber-optic light source (Schott KL-2500) fitted with a collimating lens to focus light on the coral surface (Fig. 2). The lamp was equipped with a heat filter limiting the spectral range to 400–730 nm. A temperature microsensor (TP50 microthermocouple, Unisense A/S) was mounted on a motorized micromanipulator (Märtzhäuser) with computerized depth control and was connected to a thermocouple meter (T301, Unisense). Data acquisition was done via an analog/digital converter (Unisense A/S) interfaced to a PC running software for positioning and data acquisition (Profix, Unisense A/S). The microsensor measuring tip (50 μm in diameter) was positioned onto the coral tissue or, in some experiments, was inserted into the mouth of a polyp from each coral using a dissecting microscope (Leica) before profiling commenced.

The thermal boundary layer was investigated using two hemispherical colonies (*Favia* sp. and *P. lobata*) and one branch of *S. pistillata*. Steady-state temperature profiles were measured after 10–20-min incubation at two experimental irradiances (1,080 and 2,080 μmol photons m^{-2} s^{-1}) and flow rates (0.2 cm s^{-1} and 1.3 cm s^{-1}). The effective boundary layer was determined as the intersection of the linear part of the temperature profile with the constant overlaying water temperature (*see* Jørgensen and Revsbech 1985; Fig. 1b). The convective heat flux across the boundary layer (q_{conv}) and the convection coefficient (h) were calculated using experimental estimates of ΔT and δ with Eqs. 16 and 17, respectively.

Dynamic changes in tissue temperature of hemispherical and branching corals were monitored with the temperature microsensor positioned in the polyp during light–dark shift

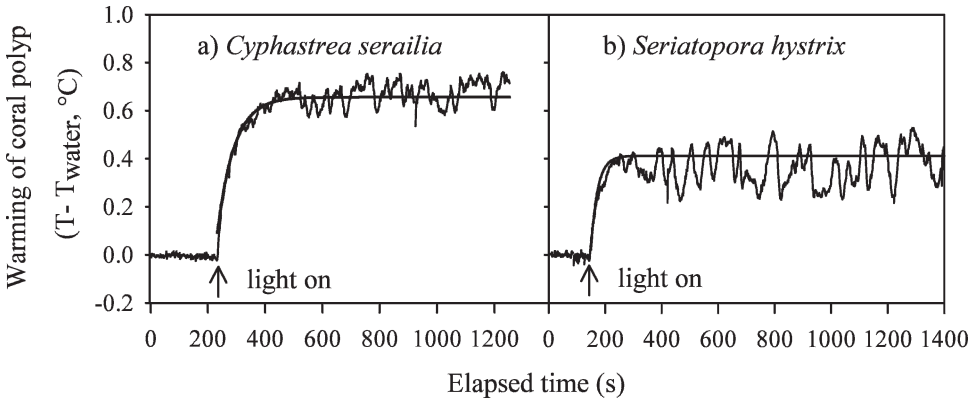

Fig. 3. Polyp warming in response to a dark–light shift. (a) Hemispherical *Cyphastrea serailia* (50 mm in diameter) and (b) thin branch of *Seriatopora hystrix* (3 mm in branch thickness).

experiments. Corals were held in the dark for 5 min before a dark–light shift was applied, using an irradiance of 2,080 μmol photons m^{-2} s^{-1} (600 W m^{-2}). The transient time constant (τ) and the steady-state surface warming (ΔT) were determined by fitting Eq. 12 to the first 600 s of the experimental heating curve.

The thermal boundary layer of one of the hemispherical corals (*Favia* sp.) was compared to the oxygen boundary layer, as measured with a Clark-type O_2 microelectrode connected to a picoamperemeter (PA2000, Unisense) and calibrated linearly using readings at air-saturated seawater and O_2-free seawater. Oxygen profiles were measured after the temperature profiles at the same flow rate (0.2 cm s^{-1}) but at lower irradiance (480 μmol photons m^{-2} s^{-1}). The thickness of the effective diffusive boundary layer was determined from the linear part of the O_2 profile (Jørgensen and Revsbech 1985), in an identical manner used to measure the thickness of the effective thermal boundary layer (described in Fig. 1b).

Solar heating—The flow chamber used in the laboratory was also set up outdoors to measure surface warming of the *P. lobata* and the *S. pistillata* specimens under direct sunlight. Water and coral surface temperature were measured with miniature thermocouples (tip diameter, 1 mm; ±0.1°C; Omega) connected to an analog-digital logger (DT-50 DataTaker Pty) calibrated against a platinum resistance Pt100 thermometer (Pyrosales Pty) in a temperature-controlled water bath (Julabo Labortechnik F10-MH). Coral surface warming was determined as the difference between coral surface temperature and water temperature after 30 min of exposure to direct sunlight. Downwelling irradiance was measured with a submersible light logger (Odyssey Dataflow Systems Pty) as photosynthetically active radiation (PAR; 400–700 nm, μmol photons m^{-2} s^{-1}). This was then converted into irradiance (W m^{-2}) using a conversion factor (0.50 W s μmol $photons^{-1}$) derived from five simultaneous measurements of irradiance (W m^{-2}) using a pyranometer (LiCor) and the PAR (μmol photons m^{-2} s^{-1}) meter, taken between 160 and 2,100 μmol photons m^{-2} s^{-1}.

In situ temperature dynamics—Temperature dynamics for specimens of *C. serailia* and *P. cylindrica* were monitored in the shallow reef flat during two 48-h periods: One with high tide occurring during the midday period (01–02 February, high tide at 11:00 h) and one with low tide occurring during midday (10–11 February, low tide at 14:00 h).

The temperature of coral skeletons and surrounding water was measured every 15 min with custom-made miniature thermistors (tip diameter, 1.5 mm; accuracy, ±0.1°C) connected to a stand-alone submersible data logger (Lothlorien Pty) and calibrated as previously described for the thermocouples. Two-millimeter holes were drilled into each of the eight coral skeletons from the side and vertically in order to place the thermistor tip at 5 mm ± 1 mm below the sun-exposed surface of coral colonies. For *P. cylindrica*, horizontally oriented branches were chosen. Additional thermistors were placed in the water column 20 mm above coral surface, out of the boundary layer. Downwelling irradiance at the depth of corals was measured as PAR, as described above.

Results

Transient response—The transient thermal model (Eqs. 9 and 12) predicts that following a sudden onset of light, the coral temperature exponentially approaches a final value and that the rate of increase is characterized by a time constant, τ, which is proportional to the coral's heat capacity (ρcV; i.e., its thermal mass) and inversely proportional to the efficiency of heat removal by convection (i.e., by water flow [AK_3h]) (Eq. 11). The temperature response of polyp tissue to a dark–light transition is shown in Fig. 3. After the onset of light, polyp warming rapidly approached a new steady state value, ΔT_m, and good fits were found between the mathematical formulation (Eq. 12) and the experimental heating curves for all investigated corals ($r^2 > 0.90$). This validates the model, whereby the temperature response of the tissue is of exponential form, although the fit was closer for the temperature curves of the hemispherical corals ($r^2 = 0.98$) compared to the thin

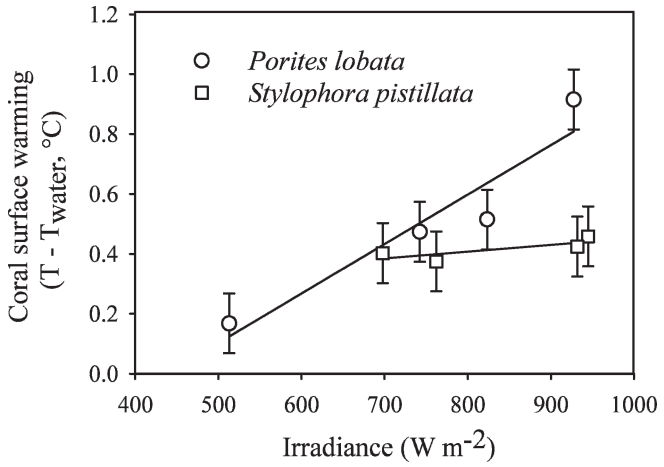

Fig. 4. Surface warming of branching *Stylophora pistillata* and hemispherical *Porites lobata* placed in a flow chamber (0.2 cm s^{-1}) under direct solar irradiance.

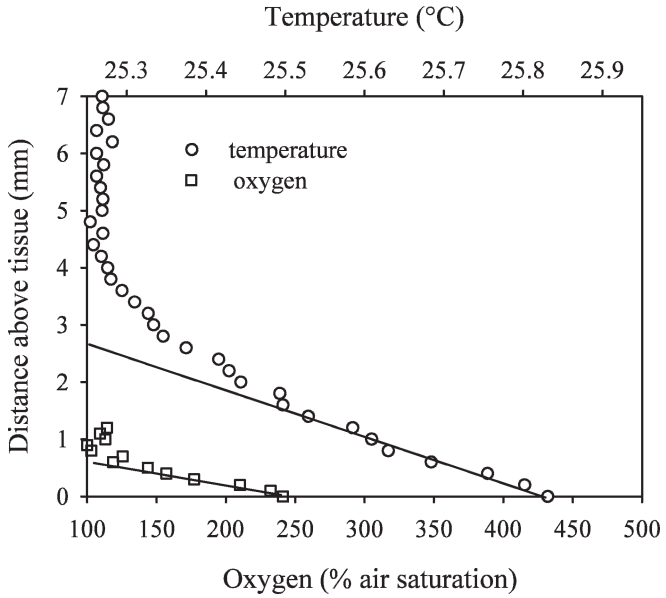

Fig. 5. Temperature and oxygen boundary layers for the hemispherical coral *Favia* sp., measured in a flow chamber (0.2 cm s^{-1}) under artificial light. Temperature (0.2 cm s^{-1}; 2,080 μmol photons m^{-2} s^{-1}); oxygen (0.2 cm s^{-1}; 480 μmol photons m^{-2} s^{-1}).

branching corals (r^2 = 0. 92). The steady-state temperature difference ΔT_m was significantly higher for the hemispherical corals (0.78°C ± 0.05°C) than for the branching corals (0.44°C ± 0.03°C) (p = 0.002; Student's t-test). The time constant (τ) of the transient heating curve was also significantly greater for the hemispherical than for the branching corals (58 ± 5 s and 26 ± 6 s, respectively; p = 0.015; Student's t-test).

Steady-state experiments—The steady-state thermal model (Eq. 13) predicts that coral surface warming is a linear function of irradiance (E). The slope of the relationship between coral surface warming and irradiance is α/K_0h and represents the relative efficiency of light absorption (α) and heat removal by convection (i.e., by water flow [h]). Figure 4 shows the experimental effect of irradiance on surface warming of hemispherical *P. lobata* colonies and of *S. pistillata* branches placed in a flow chamber at very low flow (0.2 cm s^{-1}) and exposed to direct sunlight (from approximately 1,000 to 2,000 μmol photons m^{-2} s^{-1}). The data show a linear relation between coral surface warming and irradiance for both species and for both growth forms, thus supporting the outcome of the model (r^2 = 0.89 for *P. lobata* and 0.63 for *S. pistillata*). At high irradiance (950 W m^{-2}, equivalent to 2,000 μmol photons m^{-2} s^{-1}) there was a stronger warming of the hemispherical *P. lobata* than of the branching *S. pistillata* (+0.9°C and +0.4°C, respectively) (Fig. 4), as expected from our model and theoretical estimates of the convection coefficient (h) and the tissue absorptivity (α) (*see* Discussion).

Thermal boundary layer—A comparison of thermal and diffusive boundary layers above a polyp of *Favia* sp. is shown in Fig. 5. At a flow of 0.2 cm s^{-1} and an irradiance of 480 μmol photons m^{-2} s^{-1}, zooxanthellae photosynthesis resulted in a build-up of O_2 inside the polyp of ~240% air saturation. Under identical flow and at an irradiance of 2,080 μmol photons m^{-2} s^{-1} (equivalent to 600 W m^{-2}), light absorption resulted in a 0.6°C increase in polyp temperature, compared to ambient water. The thickness of the effective thermal boundary layer was 2.6 mm, whereas the thickness of the effective diffusive boundary layer for oxygen was 0.6 mm.

An increase in flow velocity from 0.2 cm s^{-1} to 1.3 cm s^{-1} resulted in a decrease in the thickness of the thermal boundary layer (i.e., an increasing convection coefficient, h, and a decrease in tissue warming) (Table 3; Fig. 6) for all three corals (*Favia* sp., *P. lobata*, *S. pistillata*). This effect was less pronounced for *P. lobata*, which had the greatest warming (+0.6°C) of the three corals and, as predicted from the theory (Eq. 4), the strongest convective heat flux (>160 W m^{-2}). Although all three corals were exposed to the same conditions of flow and irradiance, the *S. pistillata* branch experienced the least tissue warming (Table 3), in accordance with the theoretical prediction (*see* Discussion).

The process by which a change in irradiance affects coral surface temperature is demonstrated by temperature profiles measured on a *P. lobata* specimen (Fig. 7). Following a twofold increase in irradiance, the slope of the linear part of the temperature profile doubled. This translated into a doubling in the convective heat flux q_{conv} (Table 4; Eq. 16), thus illustrating how energy inflow (i.e., absorbed irradiance) sets the value of energy outflow (i.e., convection to the ambient water) according to the heat balance (Eq. 1). Furthermore, the twofold increase in irradiance resulted in a twofold increase in tissue warming (Table 4), which further supports the linear relationship predicted by the steady-state thermal model (Eq. 13) and demonstrated in the outdoor flow chamber experiment (Fig. 4).

Table 3. Effect of flow on coral surface warming (ΔT), boundary layer thickness (δ), convective heat flux (Q), and convection coefficient (h) of the hemispherical corals *Favia* sp. and *Porites lobata* and the branching *Stylopora pistillata*. Mean ± standard error (SE) (n=3).

	Favia sp.		*S. pistillata*		*P. lobata*	
Parameter	0.2 cm s^{-1}	1.3 cm s^{-1}	0.2 cm s^{-1}	1.3 cm s^{-1}	0.2 cm s^{-1}	1.3 cm s^{-1}
ΔT (°C)	0.56±0.01	0.35±0.01	0.38±0.03	0.16±0.01	0.60±0.14	0.57±0.01
δ (mm)	2.6±0.15	1.7±0.07	3.0±0.1	1.5±0.06	2.25±0.35	1.8±0.00
Q (W m^{-2})	138±5	128±6	82±2	69±1	163±13	194±2
h (W m^{-2} K^{-1})	245±6	361±11	213±19	455±49	277±44	342±0

In situ temperature dynamics—We measured diel variations in water temperature (Fig. 8e,f) and downwelling PAR at the level of the investigated corals (Fig. 8c,d) for a period of daytime low tide (10–11 February 2006) and daytime high tide (01–02 February 2006). On 10–11 February 2006 (low tide at 14:30 h on 10 February and at 15:00 h on 11 February), the water was warmer (28.8°C ± 2.0°C) than on 01–02 February (27.4°C ± 1.0°C, high tide at 11:00 h on 01 February and at 11:30 h on 02 February) and was characterized by a greater temperature range (7.3°C and 4°C for 10–11 February and 01–02 February, respectively) and greater heating rate during the daylight period (approximately 1°C h^{-1} on 10–11 February and 0.5°C h^{-1} on 01–02 February, between 10:00 h and 16:00 h). On 10 and 11 February, water temperature reached 33.7°C ± 0.04°C and 32.4°C ± 0.12°C, respectively, toward the end of the daylight period, at approximately 16:00 h (Fig. 8e). Clear sky and water during sampling periods caused maximum recorded PAR at coral depth to reach 1,200 μmol photons m^{-2} s^{-1} on 01–02 February and 1,650 μmol photons m^{-2} s^{-1} on 10–11 February.

Diurnal variation in surface warming of the branching and the hemispherical colonies is shown in Fig. 8a and b for the two sampling periods. No warming of coral surface was detected for either of the two groups in the period of daytime high tide (01–02 February). However, on 10 and 11 February, coral surface warming occurred for both groups in the light period at low tide, and there was a significant interaction between coral shape and time of day ($p < 0.005$). The hemispherical *C. serailia* colonies (n = 4) exhibited heating of 0.3–0.6°C (10 February) and 0.3–0.5°C (11 February) relative to the mixed overlaying water. On the same days, skeletons of the branching *P. cylindrica* (n =

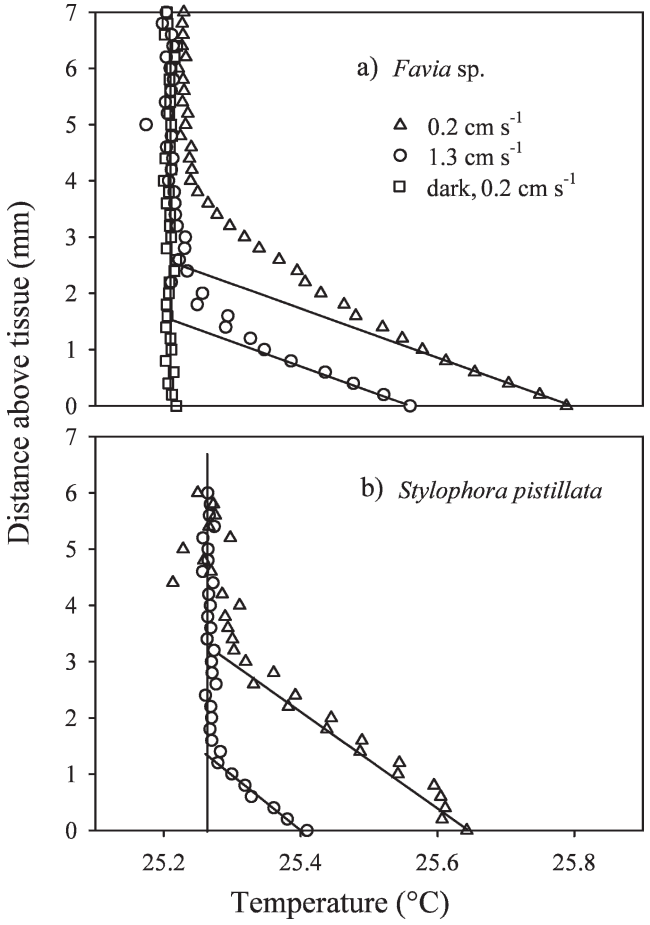

Fig. 6. Effect of flow on the temperature profile for (a) a hemispherical *Favia* sp. and (b) a branch of *Stylophora pistillata*, measured in a flow chamber and artificial light (400–730 nm, 2,080 μmol photons m^{-2} s^{-1}).

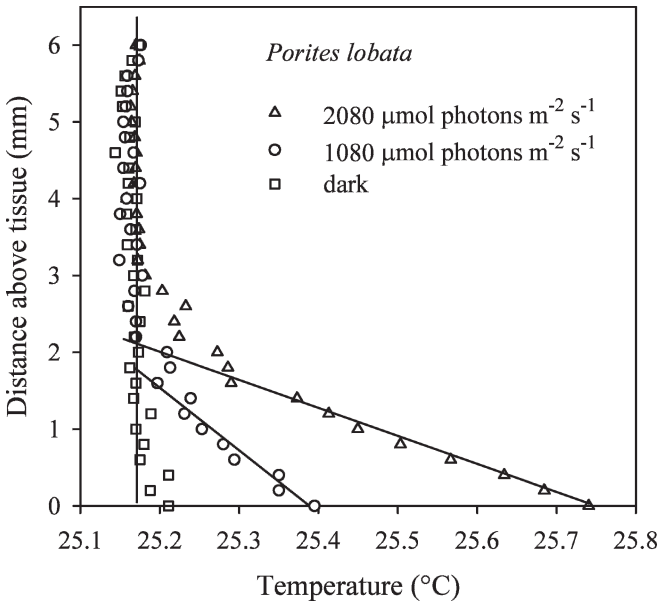

Fig. 7. Effect of irradiance on the temperature profile in the thermal boundary layer above a hemispherical *Porites lobata* (n = 4), measured in a flow chamber (0.2 cm s^{-1}) under artificial light.

Table 4. Effect of irradiance on coral surface warming (ΔT), boundary layer thickness (δ), convective heat flux (Q), and convection coefficient (h) of a *Porites lobata* colony. Mean ± standard error (SE) (n=4).

	Irradiance (μmol photons m^{-2} s^{-1})	
	1,080	2,080
ΔT (°C)	0.27±0.03	0.58±0.04
Q (W m^{-2})	93±6	178±10
δ (mm)	1.8±0.3	2.0±0.3
h (W m^{-2} K^{-1})	360±32	310±23

4) were 0.1–0.3°C and 0.2–03°C warmer than the overlaying water, respectively.

The maximum warming of the corals did not coincide with maximum irradiance (around 13:00 h) but with maximum water temperature (around 16:00 h) several hours into low tide. On 10 February, solar heating at that time of day caused the hemispherical corals to reach 33.9°C ± 0.1°C and of the branching to reach 33.8°C ± 0.09°C, while water temperature reached 33.7°C ± 0.04°C. On 11 February, the coral surface temperature reached 32.7°C ± 0.08°C in the hemispherical corals and 32.5°C ± 0.07°C in the branching corals, while water temperature reached 32.4°C ± 0.12°C. On that same day, water temperature remained above 32°C (identified as a bleaching threshold for many species in the southern Great Barrier Reef; Berkelmans and Willis 1999) for approximately 80 min, and solar heating caused the surface temperature of the hemispherical and the branching corals to exceed 32°C for approximately 150 min and 140 min, respectively.

Discussion

Seawater, with its relatively high thermal conductivity and extremely high heat capacity, is an excellent heat sink. Therefore, it might intuitively seem that only extreme seawater temperatures would expose corals to thermal stress. On the contrary, our results, and those of Fabricius (2006), show that solar-driven localized heating may well be a problem for corals in many shallow situations, albeit under conditions of very low flow. In our field study, spring low tide caused the water level on Heron Island reef flat to remain below 50 cm for up to 5 h (I. Jimenez unpubl.), and cumulative insolation on the shallow water body caused temperature to rise throughout the day and to reach a maximum at the end of the daylight period. Maximal coral surface warming of 0.6°C also occurred much later in the day than solar noon and may have coincided with timing of minimum flow on the reef flat, before the lagoon was flushed with cooler oceanic water, which caused the corals to cool down. The precise range and occurrence of flow rates for which heat transfer is limited by a thermal boundary layer need to be further investigated. Fabricius (2006) reported a surface warming of 0.2–0.6°C for shallow-water corals at flow velocities of 2–6 cm s^{-1}. Although typical flows on a coral reef usually range from 10 to 30 cm s^{-1} (Helmuth et al. 1997; Sebens et al. 1997), periods of extremely low flow (<5 cm s^{-1}) are not uncommon for lagoonal habitats (Helmuth et al. 1997). In addition, flow experienced by corals on a regular basis may be much smaller than that measured several meters above the substratum. Shashar et al. (1996) found that flow over a coral reef is controlled by a 1-m–thick benthic boundary layer (BBL), which greatly reduces flow within 50 cm of the substratum. For a mainstream water velocity of 12 cm s^{-1}, the flow within the lower–50 cm region of the BBL could be as low as 2–3 cm s^{-1} (Shashar et al. 1996), comparable to our experimental flows. Additionally, the onset of bleaching is often associated with doldrums, periods of clear skies and calm weather (Gleason and Wellington 1993; Glynn 1993). The ensuing combination of low water circulation and high light penetration is directly responsible for heating shallow water bodies, but it also matches the conditions shown in this study to allow solar-driven heating of corals. In any case, with increasing evidence that corals are particularly susceptible to small upward excursions of temperature (Glynn 1996; Hoegh-Guldberg 1999), it may become essential to understand how corals heat up in shallow areas of coral reefs.

At low flow velocities, heat removal from coral tissue is limited by the presence of a thermal boundary layer. To our knowledge, this is the first study of coral TBLs. Although the sampled flows were extremely low (<2 cm s^{-1}), we were able to demonstrate the mechanism involved in the convective cooling of corals exposed to a heat load and to investigate the effects of irradiance and flow velocity on the temperature profile within the TBL. This new data, together with our model of a coral's heat budget, allowed a preliminary assessment of the major factors governing the temperature of the living tissue of corals under conditions of low flow and high irradiance. We identify three distinctive thermal regions: the TBL, the thin veneer of living tissue, and the largely dead coral skeleton beneath. We have developed a two-lump model (Gates 1980) to distinguish between processes at the coral surface (q_{rad} and q_{conv}) and the role of the skeleton as a heat sink. Although such a clear-cut distinction between the surface layer and the skeleton is likely an oversimplification, we believe that our approach adequately describes the major factors that control temperature changes in hemispherical and branching corals. In particular, we can speculate on the importance of convection to the water compared to conduction to the skeleton. The thermal conductivities of water and calcium carbonate are 0.62 and 2.1 W m^{-1} K^{-1}, respectively (Incropera and DeWitt 1996), so that the thermal conductivity of the porous skeleton k_{skel} is in the range 1–2 W m^{-1} K^{-1}. Assuming that the skeleton conductance K of a hemispherical coral of radius R and conductivity k_{skel} can be roughly estimated by $K = k_{skel}/R$ (Gates 1980) and that the convection coefficient h in a no-flow situation is $h = k_{water}/R$ (Gates 1980), then heat is expected to dissipate from the tissue layer to the skeleton and the water to a similar degree. At higher flow rates, however, convection is expected to dominate the heat budget, as h increases as the square root of flow velocity (*see* below, Eqs. 18 to 20).

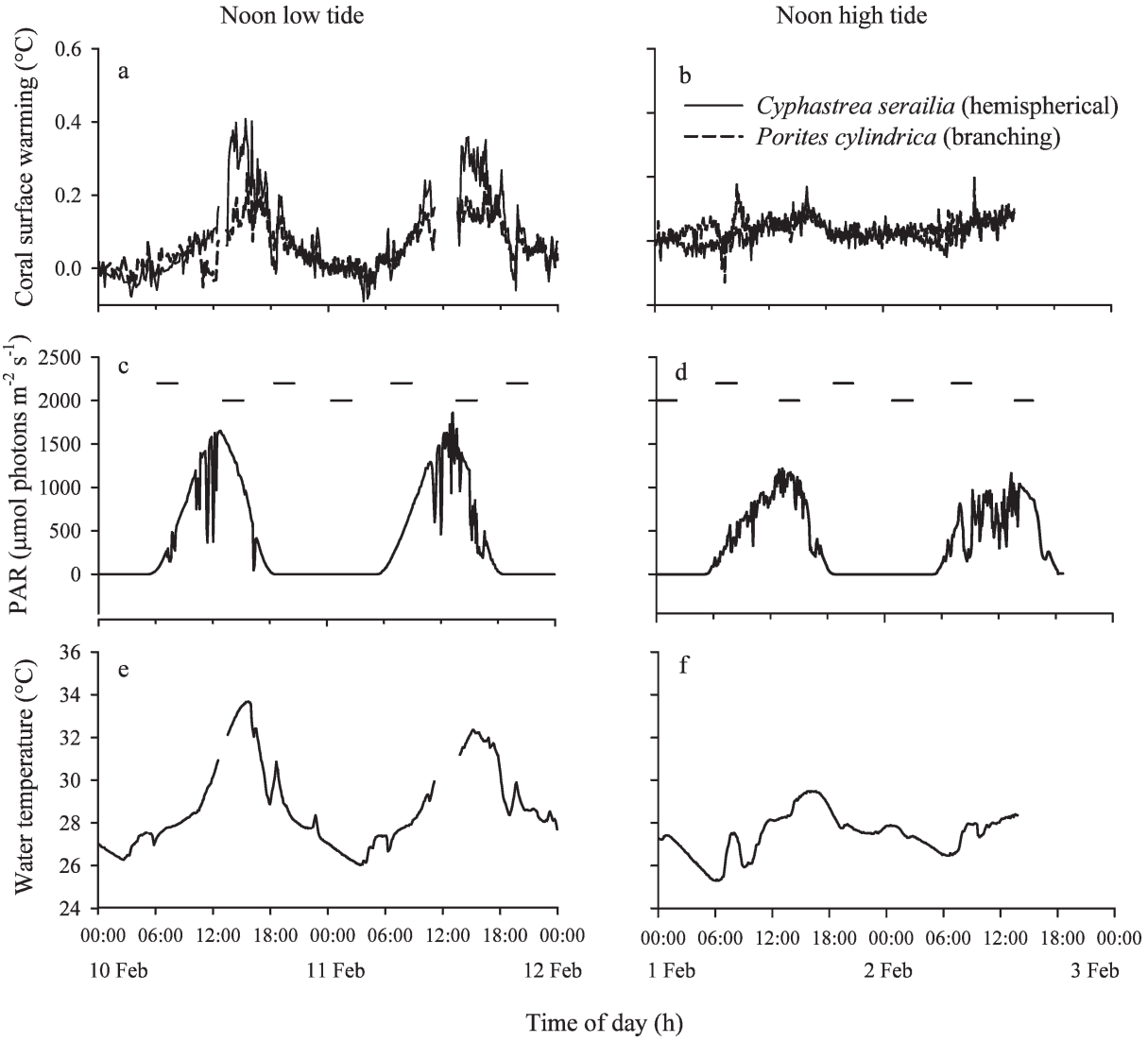

Fig. 8. In situ temperature dynamics of *Cyphastrea serailia* and *Porites cylindrica* colonies during days of noon low tide and days of noon high tide. (a, b) Temperature gradient between coral skeleton (5 mm in depth) and water. (c, d) Incident PAR at the depth of the corals for the corresponding days. The horizontal lines above the curve represent 2-h intervals centered on the time of high tide (upper series) and low tide (lower series). (e, f) Bulk water temperature.

Boundary layers—We showed that the TBL thickness of corals is in the range of 1–3 mm at low flow (<1.5 cm s^{-1}). As a comparison, DBL thicknesses of 100–1,000 μm exist for oxygen, depending on the local topography of the coral surface and the flow conditions (Shashar et al. 1993; Kühl et al. 1995; De Beer et al. 2000). The ratio of the TBL and DBL thickness ($\delta_{thermal}/\delta_{diffusion}$) is theoretically set by a dimensionless parameter, the Lewis number, which is the ratio of thermal and mass diffusivities ($Le = \alpha/D$). Theoretically, $\delta_{thermal}/\delta_{diffusion} = Le^{1/3}$. In water at 25°C the diffusivity of heat (α) is 1.4×10^{-7} m^2 s^{-1} and two orders of magnitude greater than that of O_2 ($D = 1.98 \times 10^{-9}$ m^2 s^{-1}) (Incropera and DeWitt 1996). Therefore, the TBL of aquatic organisms is predicted to be four times thicker than the DBL for oxygen. For the hemispherical coral *Favia* sp., we found a ratio of $\delta_{thermal}/\delta_{diffusion}$ = 2.6 mm/0.6 mm = 4.3 (Fig. 5), which is in close agreement with the theory. We conclude that significant boundary layers exist for heat as well as for mass transfer, indicating that thermal boundary layers may substantially affect the heat exposure of coral tissue and potentially enhance the harmful effects of hyperoxic conditions and limited toxin removal as a result of low water flow (Nakamura and Van Woesik 2001).

Heat and mass transfer being analogous processes, knowledge of DBLs can in theory be translated into estimates of TBLs, and vice versa (Incropera and DeWitt 1996), so that valuable indirect insight into the TBLs of corals could be derived from previous studies of oxygen DBLs (Shashar et al. 1993; Kühl et al. 1995; De Beer et al. 2000). Shashar et al. (1993) showed that the coral surface topography resulted in a thicker DBL over polyps than

coenosarc tissue (viz. the coral tissue that interconnects the polyps). Whether the same is true for TBLs remains to be explored and could have implications for the microscale temperature distribution at the surface of corals.

Combined microsensor analysis of thermal and diffusive boundary layers is a powerful technique to verify the strength of the heat–mass transfer analogy in the case of corals and other highly pigmented systems, such as, for example, microbial mats and sediments. The presence of a microsensor can induce a local compression of the diffusive boundary layer (Glud et al. 1994), most likely as a result of a local acceleration of the flow. This could create an artefact in our data, but we would expect a similar effect on both temperature and oxygen microprofiles. More detailed investigations are required to test the importance of boundary layer compression.

Influence of flow rate—Flow velocity affects coral temperature by thinning the TBL, thereby reducing the resistance to heat transfer toward the water and resulting in an increase in the convection coefficient, h (Table 3; Fig. 6). Theoretical guidelines from classical treatments of heat transfer, together with predictions from our model (Eq. 13), can be used to estimate coral surface warming at higher and lower flow rates. The effect of flow velocity (v) on convection is traditionally expressed in terms of two dimensionless parameters from heat transfer engineering (Incropera and DeWitt 1996), the well-known Reynolds number (Re):

$$Re = vL/v \tag{18}$$

where v is the kinematic viscosity of water and L is the characteristic dimension of the organism, and the Nusselt number (Nu), which is the ratio of heat transfer assisted by water motion to that with conduction alone:

$$Nu = hL/k \tag{19}$$

where k is the conductivity of water. The effect of flow on convection is expressed as an empirically derived relationship of the form $Nu = c\ Re^m$, in which the exponent m is specific to the shape of the submerged object and is known for simple geometrical shapes such as spheres (Incropera and DeWitt 1996). For $Re < 7.6\times10^4$:

$$Nu = 2 + 2.03\left(0.4\,Re^{0.5} + 0.06\,Re^{0.67}\right) \tag{20}$$

Thus, a 5-cm–diameter sphere in a 5 cm s^{-1} flow would have a convection coefficient (h) of 875 W m^{-2} K^{-1}. The resulting surface warming, given by Eq. 13, is thus $\Delta T_{m\,tissue} = 0.14$°C (assuming E is 600 W m^{-2}; α is approximately 0.2 (*see* later), and where for high values of h the constant K_0 can be shown to be close to 1).

On the other hand, in the extreme no-flow situation, heat exchange with the surrounding water would occur by conduction alone, and the convection coefficient (h) in Eq. 13 would be replaced by a conduction coefficient (h_{cond}), which depends only on the conductivity of water (k; 0.616 W K^{-1} m^{-2}) and the coral diameter (L; for example, 5 cm): $h_{cond} = 2k/L = 25$ W m^{-2} (Denny 1993). In this case, Eq. 13 predicts a surface warming $\Delta T_{m\,tissue} = 2.75$°C (where E and α are 600 W m^{-2} and 0.2, respectively, and where for small values of h the constant K_0 can be shown to be approximately $2 - A_1/A$, where A_1/A is the fraction of surface area that intercepts the direct light beam and is estimated as the ratio of a sphere's cross section [$A_1 = \pi(d/2)^2$] with its total surface area [$A = 4\pi(d/2)^2$]; i.e., 1/4). These considerations indicate that under extreme conditions of no flow and high irradiance (>1,000 μmol photons m^{-2} s^{-1}), shallow-water corals could experience temperatures up to 3°C higher than the surrounding water.

Size and shape of corals—The corals investigated in this study can be roughly divided into hemispherical types (>5 cm) and thinly branched corals (branch diameter up to a few cm). In all experiments, the larger hemispherical colonies experienced higher surface warming than the thin branches. Equations 18 through 20 predict that h decreases with coral size as $d^{-0.5}$, thus indicating that the size of corals is a critical factor potentially affecting heat fluxes and surface temperature. The effect of coral shape can also be discussed using engineering theory of heat transfer. The dimensionless *Nu*-*Re* relationship for a cylinder in laminar flow and low velocity ($Re < 4{,}000$) (Incropera and DeWitt 1996) is

$$Nu = 1.23\,Re^{0.466} \tag{21}$$

Therefore, theoretically derived values of the convection coefficient (h; Eq. 19) would be 700, 300, and 370 W m^{-2} K^{-1} for cylinders 10 mm in diameter and 50 mm in diameter and a sphere 50 mm in diameter (Eq. 20), respectively, placed in a 1 cm s^{-1} cross flow. A thin (10-mm–diameter) coral branch would thus exchange heat with the surrounding water twice as efficiently as a thicker branch (50 mm in diameter) or a larger hemispherical (50 mm in diameter) coral. Although this is consistent with previous mass transfer studies (Nakamura and Van Woesik 2001; Falter et al. 2007), the results from our boundary layer study did not show such a difference in the local convection coefficient (h) between the branching *S. pistillata* and the hemispherical *P. lobata* and *Favia* sp. at the flows tested (Table 3). However, the reduction in TBL thickness that resulted from an increase in flow appeared more pronounced for the branching coral than for the hemispherical colonies (Table 3; Fig. 6). There is clearly a need for further investigation of coral shape factors and their importance for coral heat budgets.

Our first results indicate that the temporal response of corals exposed to fluctuating environmental conditions may also be affected by coral shape and/or size. The time constant (τ) of the transient heating curve of the hemispherical corals was twice that of the thin branches. τ is a measure of the rapidity of the coral's thermal response following a sudden increase in irradiance or water temperature: Eq. 12 states that after a time equal to the constant τ, coral surface warming (ΔT) has reached $(1 - e^{-1})\Delta T_m$; i.e., $0.63 \times \Delta T_m$. In other words, the time constant τ is the time it takes for coral warming to reach 63% of the final value ΔT_m. The smaller the time constant, the faster the coral heats up after onset of light.

Our model (Eq. 11) predicts that τ is inversely proportional to the coral's surface area to volume ratio (A/V). For a sphere and a cylinder of radius r this is $3/r$ ($[4\pi r^2]/[(4/3)\pi r^3]$) and $2/r$ ($[L2\pi r]/[L\pi r^2]$), respectively. Therefore, τ of hemispherical and cylindrical corals increases proportionally to the coral radius (as $r/3$ and $r/2$, respectively). Although the response time of spheres and cylinders of equally small diameter are not expected to differ significantly, larger massive colonies are likely to have a much slower temporal response than thin branches. Our first data set indicates that the surface layer of small corals (<5 cm) have response times shorter than 1 min, and our model indicates that this could increase for large (1-m) massive colonies to 15 min. The skeleton of larger colonies could therefore potentially dampen the temperature response to rapid environmental fluctuations, such as light flecks, cloud passage, or rapid fluctuations in flow rate. Our theoretical considerations indicate that the size more than the shape (cylinder vs. sphere) accounts for differences in surface warming between small branches and larger massive colonies.

The magnitude of warming reached in the steady state is determined by the balance between the amount of light energy absorbed by coral tissue and the efficiency of heat removal by convection to the water column (Eqs. 10 and 13). Fabricius (2006) provided strong evidence that coral pigmentation is a key factor determining the surface temperature of corals. Pigmentation is quantified in our model by the tissue's absorptivity (α), an estimate of which can be derived from Eq. 13, and using the known value of irradiance, E (2,080 μmol photons m^{-2} s^{-1}), the empirical values of ΔT, and the convection coefficient, h (Table 3). For the three corals *Favia* sp., *P. lobata*, and *S. pistillata* we found α values of 0.23, 0.28, and 0.13, respectively. This estimation neglects heat transfer to the skeleton for the time being ($K = 0$, thus $K_0 = 1$ in Eq. 13) and thus presents an overestimation. We speculate that the branching coral *S. pistillata* may therefore have had a smaller light-absorbing capacity than the hemispherical colonies *Favia* sp. and *P. lobata*, possibly as a result of a thinner tissue or lower pigment content. There is a need to further investigate the efficiency of heat absorption for hemispherical and branching corals. In our study all sampled surfaces were oriented perpendicularly to the incident light. In the field, however, the orientation of the tissue relative to the incident irradiance would greatly affect absorption, especially for vertically oriented branches. At the scale of a single branch, this would appear in our model as a correction to the incident irradiance E of the form $E \cos \theta$, where θ is the angle between the direct incident light beam and the direction normal to the surface (Gates 1980). The surface warming ΔT_{tissue} would thus be proportionally reduced by $\cos \theta$ (Eq. 13). Therefore, geometrical as well as biological characteristics of corals may affect their surface heat budget.

Implications for mass coral bleaching—Bleaching is often more severe in shallow environments (Marshall and Baird 2000), during doldrums or periods of low wind and calm seas, when light penetration is strong (Glynn 1993, 1996). Additionally, corals often bleach first on their uppermost surface (Williams and Bunkley-Williams 1990). Thus, both elevated sea temperature and solar radiation concur in triggering natural bleaching events (Fitt and Warner 1995; Glynn 1996; Brown 1997), and the synergistic effect of high temperature and radiation cause damage to the photosynthetic mechanisms of the zooxanthellae (Lesser 1996; Jones et al. 1998; Hill and Ralph 2006). Our results and those of Fabricius (2006) indicate an additional effect of light, in that the mere heating power of solar radiation can contribute to increases in the heat load of exposed coral tissue. Both PAR (400–700 nm) and ultraviolet radiation (280–400 nm) have been implicated in triggering bleaching (Gleason and Wellington 1993; Brown et al. 1994; Fitt and Warner 1995). Which waveband contributes more to a coral's heat budget is likely to depend on the spectral distribution of light reaching corals (the shorter wavelengths carrying higher energy) and the coral tissue absorptivity, α.

Solar heating of shallow-water corals could have profound implications for bleaching. In summer, corals live close to their upper thermal limit, and increases in temperature as small as 1–2°C above the mean monthly summer temperature can trigger bleaching (Berkelmans and Willis 1999). Both the absolute temperature rise above the threshold and the duration of exposure affect the severity of a bleaching event (Gleeson and Strong 1995; Winter et al. 1998; Berkelmans 2002). Therefore, the severity of bleaching events is predicted based on a cumulative stress index (i.e., degree heating weeks [DHW], which represents the accumulation of anomalously high sea surface temperature on reefs) (Liu et al. 2003): One DHW represents either a +1°C anomaly lasting 1 week or a +2°C anomaly lasting half a week. A value of 8 DHW is known to trigger mass coral bleaching (Liu et al. 2003). Such indices may need to be evaluated in light of the present results showing that although corals may be exposed to a water body at uniform temperature, differential effects of solar heating may cause some corals to exceed the maximum expected summertime temperature for a longer period of time, and by a larger amount than others.

It is well documented that branching corals often are more sensitive to thermal stress than are massive coral species (Marshall and Baird 2000; Loya et al. 2001). Shape-related differences in coral thermal exposure could explain some of the observed differences in bleaching susceptibility among taxa. Corals living in reef environments that frequently experience extreme temperatures may be more resistant to bleaching conditions compared to corals living in more stable physical environments (Jokiel and Coles 1990; Glynn 1996; Marshall and Baird 2000). Brown et al. (2000, 2002) also showed that the bleaching tolerance of corals can be shaped by their experience of exposure to solar radiation. Our results indicate that large hemispherical colonies experience higher temperatures than thin branching corals. How this affects their resistance to bleaching remains to be investigated.

In summary, we have shown that microscale temperature measurements coupled with theoretical analysis using

well-known concepts from heat and mass transfer theory can yield important insights into the regulation of coral heat budgets. In combination with more detailed studies of the optical properties of corals and their energy metabolism (e.g., with fiber-optic microsensors; Kühl 2005), this approach may even allow the construction of a complete energy budget for particular corals.

References

Atkinson, M., and R. Bilger. 1992. Effects of water velocity on phosphate uptake in coral reef-flat communities. Limnol. Oceanogr. **37:** 273–279.

Berkelmans, R. 2002. Time-integrated thermal bleaching thresholds of reefs and their variation on the Great Barrier Reef. Mar. Ecol. Prog. Ser. **229:** 73–82.

———, and B. L. Willis. 1999. Seasonal and local spatial patterns in the upper thermal limits of corals on the inshore Central Great Barrier Reef. Coral Reefs **18:** 219–228.

Brown, B. E. 1997. Coral bleaching: Causes and consequences. Coral Reefs **16:** 129–138.

———, R. P. Dunne, M. S. Goodson, and A. E. Douglas. 2000. Bleaching patterns in reef corals. Nature **404:** 142–143.

———, ———, ———, and ———. 2002. Experience shapes the susceptibility of a reef coral to bleaching. Coral Reefs **21:** 119–126.

———, ———, T. P. Scoffin, and M. D. A. Letissier. 1994. Solar damage in intertidal corals. Mar. Ecol. Prog. Ser. **105:** 219–230.

Coles, S. L., and B. E. Brown. 2003. Coral bleaching—capacity for acclimatization and adaptation. Adv. Mar. Biol. **46:** 183–223.

Dade, W. B., A. J. Hogg, and B. P. Boudreau. 2001. Physics of flow above the sediment-water interface, p. 4–43. *In* B. P. Boudreau and B. B. Jørgensen [eds.], The benthic boundary layer: Transport processes and biogeochemistry. Oxford Univ. Press.

De Beer, D., M. Kühl, N. Stambler, and L. Vaki. 2000. A microsensor study of light enhanced Ca^{2+} uptake and photosynthesis in the reef-building coral *Favia* sp. Mar. Ecol. Prog. Ser. **194:** 75–85.

Dennison, W. C., and D. J. Barnes. 1988. Effect of water motion on coral photosynthesis and calcification. J. Exp. Mar. Biol. Ecol. **115:** 67–77.

Denny, M. W. 1993. Air and water: The biology and physics of life's media. Princeton Univ. Press.

Enriquez, S., E. R. Mendez, and R. Iglesias-Prieto. 2005. Multiple scattering on coral skeletons enhances light absorption by symbiotic algae. Limnol. Oceanogr. **50:** 1025–1032.

Fabricius, K. E. 2006. Effects of irradiance, flow, and colony pigmentation on the temperature microenvironment around corals: Implications for coral bleaching? Limnol. Oceanogr. **51:** 30–37.

Falter, J. L., M. J. Atkinson, R. J. Lowe, S. G. Monismith, and J. R. Koseff. 2007. Effects of nonlocal turbulence on the mass transfer of dissolved species to reef corals. Limnol. Oceanogr. **52:** 274–285.

Finelli, C., B. Helmuth, N. Pentcheff, and D. Wethey. 2006. Water flow influences oxygen transport and photosynthetic efficiency in corals. Coral Reefs **25:** 47–57.

Fitt, W. K., and M. E. Warner. 1995. Bleaching patterns of four species of Caribbean reef corals. Biol. Bull. **189:** 298–307.

Gates, D. M. 1980. Biophysical ecology. Courier Dover Publications.

Gleason, D. F., and G. M. Wellington. 1993. Ultraviolet radiation and coral bleaching. Nature **365:** 836–838.

Gleeson, M. W., and A. E. Strong. 1995. Applying MCSST to coral reef bleaching. Adv. Space Res. **16:** 151.

Glud, R., J. Gundersen, N. Revsbech, and B. Jørgensen. 1994. Effects on the benthic diffusive boundary layer imposed by microelectrodes. Limnol. Oceanogr. **39:** 462–467.

Glynn, P. W. 1993. Coral reef bleaching: Ecological perspectives. Coral Reefs **12:** 1–17.

———. 1996. Coral reef bleaching: Facts, hypotheses and implications. Glob. Change Biol. **2:** 495–509.

Helmuth, B. S. T., B. E. H. Timmerman, and K. P. Sebens. 1997. Interplay of host morphology and symbiont microhabitat in coral aggregations. Mar. Biol. **130:** 1–10.

Hill, R., and P. J. Ralph. 2006. Photosystem II heterogeneity of *in hospite* zooxanthellae in scleractinian corals exposed to bleaching conditions. Photochem. Photobiol. **82:** 1577–1585.

Hoegh-Guldberg, O. 1999. Climate change, coral bleaching and the future of the world's coral reefs. Mar. Freshw. Res. **50:** 839–866.

Incropera, F. P., and D. P. Dewitt. 1996. Fundamentals of heat and mass transfer, 4th ed. Wiley.

Jokiel, P. L., and S. L. Coles. 1990. Response of Hawaiian and other Indo-Pacific reef corals to elevated temperature. Coral Reefs **8:** 155–162.

Jones, R. J., O. Hoegh-Guldberg, A. W. D. Larkum, and U. Schreiber. 1998. Temperature-induced bleaching of corals begins with impairment of the CO_2 fixation metabolism in zooxanthellae. Plant Cell Environ. **21:** 1219–1230.

Jørgensen, B. B. 2001. Life in the diffusive boundary layer, p. 348–373. *In* B. P. Boudreau and B. B. Jørgensen [eds.], The benthic boundary layer: Transport processes and biogeochemistry. Oxford Univ. Press.

———, and D. J. Des Marais. 1990. The diffusive boundary layer of sediments: Oxygen microgradients over a microbial mat. Limnol. Oceanogr. **35:** 1343–1355.

———, and N. P. Revsbech. 1985. Diffusive boundary layers and the oxygen uptake of sediments and detritus. Limnol. Oceanogr. **30:** 111–122.

Koch, E. W., J. D. Ackerman, J. Verduin, and M. Van Keulen. 2006. Fluid dynamics in seagrass ecology—from molecules to ecosystems, p. 193–225. *In* A. W. D. Larkum, R. J. Orth, and C. M. Duarte [eds.], Seagrasses: Biology, ecology and conservation. Springer Verlag.

Kühl, M. 2005. Optical microsensors for analysis of microbial communities. Meth. Enzymol. **397:** 166–199.

———, Y. Cohen, T. Dalsgaard, J. B. Barker, and N. P. Revsbech. 1995. Microenvironment and photosynthesis of zooxanthellae in scleractinian corals studied with microsensors for O2, pH and light. Mar. Ecol. Prog. Ser. **117:** 159–172.

Larkum, A. W. D., E.-M. W. Koch, and M. Kühl. 2003. Diffusive boundary layers and photosynthesis of the epilithic algal community of coral reefs. Mar. Biol. **142:** 1073–1082.

Lesser, M. P. 1996. Elevated temperatures and ultraviolet radiation cause oxidative stress and inhibit photosynthesis in symbiotic dinoflagellates. Limnol. Oceanogr. **41:** 271–283.

———, V. M. Weis, M. R. Patterson, and P. L. Jokiel. 1994. Effects of morphology and water motion on carbon delivery and productivity in the reef coral, *Pocillopora damicornis* (Linnaeus): Diffusion barriers, inorganic carbon limitation, and biochemical plasticity. J. Exp. Mar. Biol. Ecol. **178:** 153–179.

Liu, G., A. E. Strong, and W. J. Skirving. 2003. Remote sensing of sea surface temperatures during 2002 barrier reef coral bleaching. EOS Trans. Am. Geophys. Union **84:** 137–141.

Loya, Y., K. Sakai, K. Yamazato, Y. Nakano, H. Sambali, and R. Van Woesik. 2001. Coral bleaching: The winners and the losers. Ecol. Lett. **4:** 122–131.

Marshall, P. A., and A. H. Baird. 2000. Bleaching of corals on the Great Barrier Reef: Differential susceptibilities among taxa. Coral Reefs **19:** 155–163.

Nakamura, T., and R. Van Woesik. 2001. Water-flow rates and passive diffusion partially explain differential survival of corals during the 1998 bleaching event. Mar. Ecol. Prog. Ser. **212:** 301–304.

Patterson, M. R. 1991. The effects of flow on polyp-level prey capture in an octocoral, *Alcyonium siderium*. Biol. Bull. **180:** 93–102.

———. 1992. A mass-transfer explanation of metabolic scaling relations in some aquatic invertebrates and algae. Science **255:** 1421–1423.

Sebens, K. P., J. Witting, and B. Helmuth. 1997. Effects of water flow and branch spacing on particle capture by the reef coral *Madracis mirabilis* (Duchassaing and Michelotti). J. Exp. Mar. Biol. Ecol. **211:** 1–28.

Shashar, N., Y. Cohen, and Y. Loya. 1993. Extreme diel fluctuations of oxygen in diffusive boundary layers surrounding stony corals. Biol. Bull. **185:** 455–461.

———, S. Kinane, P. Jokiel, and M. Patterson. 1996. Hydromechanical boundary layers over a coral reef. J. Exp. Mar. Biol. Ecol. **199:** 17–28.

Shick, J. M. 1990. Diffusion limitation and hyperoxic enhancement of oxygen consumption in zooxanthellate sea anemones, zoanthids, and corals. Biol. Bull. **179:** 148–158.

Williams, E. J., and L. Bunkley-Williams. 1990. The world-wide coral reef bleaching cycle and related sources of coral mortality. Atoll Res. Bull. **355:** 1–72.

Winter, A., R. S. Appeldoorn, A. Bruckner, E. H. Williams, Jr., and C. Goenaga. 1998. Sea surface temperatures and coral reef bleaching off La Parguera, Puerto Rico (northeastern Caribbean Sea). Coral Reefs **17:** 377–382.

Received: 15 May 2007
Accepted: 25 March 2008
Amended: 25 February 2008